Journal of Hydrology 572 (2019) 692–705

Contents lists available at ScienceDirect

Journal of Hydrology

journal homepage: www.elsevier.com/locate/jhydrol

Research papers

Improving the representation of stomatal responses to CO_2 within the Penman–Monteith model to better estimate evapotranspiration responses to climate change

Xiaojie Li, Shaozhong Kang*, Jun Niu, Zailin Huo, Junzhou Liu

Center for Agricultural Water Research in China, China Agricultural University, Beijing 100083, China

ARTICLE INFO

This manuscript was handled by Marco Borga, Editor-in-Chief, with the assistance of Sergio M. Vicente-Serrano, Associate Editor

Keywords:
Stomatal conductance
CO_2 concentration
Linear model
Hyperbolic model
Modified hyperbolic model
Evapotranspiration
Penman–Monteith

ABSTRACT

An increase in atmospheric CO_2 concentration (CO_2) affects stomatal conductance (g_s). Since g_s is an important parameter in the Penman–Monteith model (P-M), an accurate estimate of g_s can improve the accuracy of the estimation of evapotranspiration (*ET*) by P-M when CO_2 increases. This paper identifies three models of the relationship between g_s and CO_2 (the *linear model*, L, the *hyperbolic model*, H, and the *modified hyperbolic model*, MH), and compares their estimations of *ET* when they are incorporated into P-M. A two-year experiment which included four levels (400, 550, 700, and 900 μmol mol^{-1}) and three levels (400, 550, and 700 μmol mol^{-1}) of CO_2 in 2015 and 2016, respectively, was conducted in order to obtain validation data. Fifty papers that had studied the effect of increased CO_2 on g_s, over a 45-year period, were analyzed to obtain calibration data. After being calibrated and validated, each of the three models was in turn included as a component of P-M to estimate *ET* under increased CO_2, followed by the comparison between estimated and observed *ET*. The sensitivity of P-M to the parameters in three models was also analyzed. Our results show that g_s decreased and the reduction rate gradually lessened as CO_2 increased. Of the three models, MH gave the best estimate of g_s, having the largest values of the coefficient of determination (R^2), 0.97, the Nash–Sutcliffe efficiency coefficient (*NSE*), 0.96, and the modified affinity index (*d*), 0.93, and the smallest values of the root mean square error (*RMSE*), 0.03, and the Akaike information criterion (*AIC*), −47.48. Each of the three models gave different *ET* results for different levels of CO_2 when used as a component of P-M. The MH had better *ET* estimations than L and H when compared to observed *ET* across all CO_2 concentration levels, with the highest R^2, *NSE*, and *d*, and the lowest *RMSE* and *AIC*. The sensitivity of P-M to the empirical parameters varied among the three models, for instance, ± 40 and ± 20% changes of parameter *p* in L, g_{smaxp} and C_{s0} in H, and *b* in MH resulted in −15 to 4%, −13 to 7%, −9 to 4%, and −3 to 3% changes in predicted *ET*, respectively. Thus, changes of parameter *b* in MH had minimum effect on predicted *ET*, indicating greater stability of P-M in *ET* estimation by incorporating MH. Therefore, using MH to model the response of g_s to increased CO_2 when incorporated into P-M to estimate *ET* not only represents a more appropriate stomata physiological reaction to higher CO_2, but also results in a more accurate estimate of *ET*, and making the model more broadly applicable.

1. Introduction

Evapotranspiration (*ET*) is an important parameter in farmland irrigation management and an important part of the hydrologic cycle. Accurate estimation of *ET* can help to increase the conservation of irrigation water and manage water resources in a river basin (Bastiaanssen et al., 2005; Kang et al., 2003). Among many models that estimate *ET*, a combination method called the Penman–Monteith (P-M) model (Monteith, 1965), which schematizes the vegetation cover as a single big leaf at a certain height, has been widely used both in farmland *ET* estimation (Li et al., 2014; Tanasijevic et al., 2014; Wu et al., 2012; Zhang et al., 2008) and in regional hydrological models (Arnold et al., 1998; Liang et al., 1994, 1996) because of its simple form and easy parameterization.

Canopy conductance (g_c) in P-M represents the conductance of water vapor through the stomata, through the entire canopy, and from the interior of the soil to the soil surface; it is an important parameter for the estimation of *ET* (Allen et al., 1998; Jiang et al., 2016). Monteith (1965) hypothesized that g_c was the product of maximum stomatal conductance (g_{smax}) and effective leaf area index (LAI_{active}). Based on

* Corresponding author.
E-mail address: kangsz@cau.edu.cn (S. Kang).

https://doi.org/10.1016/j.jhydrol.2019.03.029
Received 14 November 2018; Received in revised form 27 February 2019; Accepted 2 March 2019
Available online 16 March 2019
0022-1694/

Monteith's work, Jarvis (1976) introduced a multi-environment factor multiplication model and created a canopy conductance model (Jarvis model) which has since been widely used (Stewart, 1988; Li et al., 2014; Lhomme et al., 1998; Zhang et al., 2008; Noilhan and Planton, 1989). In the Jarvis model, the environmental factors include net radiation (R_n), temperature (T), water vapor pressure deficit (VPD), soil water content (θ), and CO_2 concentration. The Jarvis model performed under the hypothesis that the influence of all the factors are without any synergistic interactions (Jarvis, 1976). When the time period is short, the change in atmospheric CO_2 concentration is very small and is generally ignored (Li et al., 2014; Zhang et al., 2008). However, in recent years the atmospheric concentration of CO_2 has increased because of global climate change (IPCC, 2013), which has both directly and indirectly affected agriculture and hydrology by decreasing stomatal conductance (g_s) (Morison, 1998), increasing plant height and leaf area (Kang et al., 2002), as well as changing drought and flood extrame patterns (Piao et al., 2010). As a result, more researchers are involving in the fundamental field of how the g_s responds to changes in CO_2 concentration and applying the theories in analyses of crop ET, yield, and watershed runoff under present and future climate change scenarios (Niu et al., 2013; Wang et al., 2016; Wu et al., 2012).

The relationship between g_s and atmospheric CO_2 concentration has been well documented. For example, Jarvis (1976) used a piecewise linear function to represent the relationship between them. He concluded that when the CO_2 concentration is between 100 and 1000 μmol mol^{-1}, the g_s decreased linearly as the CO_2 concentration increased, and when the CO_2 concentration is < 100 μmol mol^{-1} or > 1000 μmol mol^{-1}, the g_s was constant. Morison (1987) found a 40% decrease in g_s when the CO_2 concentration was doubled from 330 to 660 μmol mol^{-1}, which was introduced to a linear expression to model the g_s-CO_2 relationship in the Erosion Productivity Impact Calculator model (EPIC) (Easterling et al., 1992). Morison and Gifford (1983) fitted the g_s-CO_2 curves by quadratic functions in two C_3 and two C_4 species under different leaf-air vapor pressures. Ball et al. (1987) proposed an empirical–mechanistic model to simulate the relationship between g_s and CO_2 concentration, which was called Ball-Berry stomatal conductance model (Ball et al., 1987; Collatz et al., 1991). Their model included the photosynthetic rate (P_n), which is significant because it includes plant physiology in the model. Wang and Wen (2010) found that the rate of decrease of g_s gradually lessened as the CO_2 concentration increased. They analyzed the response of g_s to changes in atmospheric CO_2 concentration based on the physiological and biochemical mechanisms of stomatal activity, and produced a hyperbolic model for the response of g_s to changes in CO_2 concentration. This model was validated using nine species of plants.

But there are still some issues about those relationships mentioned above. Even though the linear relationship by Easterling et al. (1992) is the most commonly used model for estimating the effect of increased CO_2 concentration on ET using the P-M model, and has since been used in the Soil and Water Assessment Tool (SWAT) and the Variable Infiltration Capacity (VIC) model (Liang et al., 1994; Neitsch et al. 2005; Niu et al., 2013), its accuracy has not been verified. Furthermore, there were no estimates when CO_2 concentration was > 660 μmol mol^{-1}, so the reliability of using this linear model to estimate ET under higher CO_2 concentrations is unknown. In the Ball–Berry model (Ball et al., 1987; Collatz et al., 1991), P_n is calculated differently, and the calculation is complex, so the Ball–Berry model has not been applied into the P-M model to estimate the effect of increased CO_2 concentration on ET. The hyperbolic model of Wang and Wen (2010) includes physiological parameters and provides accurate estimates of g_s within nine plant species, but there is no research incorporating this model into P-M to estimate ET responses to increased CO_2 concentration. Therefore, it is important and necessary to validate the accuracy and reliability of these models when applying them into P-M to estimate ET, especially when the CO_2 concentration is higher than 660 μmol mol^{-1}, to find the best physiological and theoretic g_s-CO_2 relationships for estimating ET under climate change.

The objective of this study is to obtain an optimal model of the g_s-CO_2 relationship that is theoretically valid and that represents changes in plant physiological activity in response to higher CO_2 concentrations, so as to improve the accuracy and reliability of the estimate of ET by P-M when atmospheric CO_2 concentration increases. Therefore, in this study, the empirical parameters in the g_s-CO_2 models were calibrated using the g_s and CO_2 data collected from 50 representative journal articles and the least square method. The different model predictions were validated using the g_s and ET data derived under different CO_2 concentrations in the two-year experiment. This allows us to compare the accuracy of the g_s and ET estimated by the empirical models with the observed g_s and ET under increased atmospheric CO_2 concentration, as well as with the estimated ET by P-M model without taking the stomatal response to CO_2 into account. As each of the models was incorporated into P-M, sensitivity analysis will enable us to determine the stability of the models.

2. Materials and methods

2.1. Experimental conditions and design

The experiment was conducted in the periods May–September 2015 and April–July 2016 in a climatic phytotron at the Shiyanghe Experimental Station of China Agricultural University, located in Wuwei City, Gansu Province, Northwest China (37°52′ N, 102°50′ E, altitude 1581 m). The climatic phytotron consisted of four separate chambers, each with dimensions 3 m (length) × 4 m (width) × 2.5 m (height). The chambers were equipped identically.

Daily computer-controlled adjustments to the environmental conditions were made every 2 h in the period 8:00 h to 20:00 h. The temperature and humidity were adjusted every 10 days according to the 10-day averages of observed data from April to September that had been gathered at the experimental station over the previous six years. The experiment used natural light. The CO_2 concentrations in the chambers were supplemented by CO_2 gas cylinders and monitored by CO_2 gas analyzers. There were four CO_2 concentrations respectively in four chambers in 2015 (400, 550, 700, and 900 μmol mol^{-1}) and three CO_2 concentrations respectively in three chambers in 2016 (400, 550, and 700 μmol mol^{-1}). More details of the indoor equipment and the control principles were described by Li et al. (2018).

The crop used in the experiment was a field-grown maize cultivar (*Zea mays* L., cultivar Qiangsheng 51, C_4) which was planted in plastic pots of height 26.5 cm, bottom diameter 21 cm, and top diameter 33 cm. Each chamber had twelve pots as the trial replicates. Initially three seeds were sown in each plastic pot and one seedling was retained after emergence. The experiment was conducted in the phytotron during the period from the date of sowing (May 7 in 2015 and April 22 in 2016) to the end of the experiment (September 16 in 2015 and July 31 in 2016). Stones were spread over the bottom of each pot, with fine sand, to act as a filtration layer. The pots were filled with local sandy loam soil that had been air-dried, crushed, and sieved. Each pot contained 18 kg soil with dry bulk density of 1.38 g cm^{-3}, field water capacity of 0.27 cm^3 cm^{-3}, and wilting point of 0.10 cm^3 cm^{-3}. The surface of the soil was then covered with fine sand and nutritive soil to reduce the impact of irrigation on the topsoil structure. The pots were weighed every 3–4 days by high precision weighing scales to determine the required amount of irrigation water, and the irrigation water was measured in graduated cylinders. The average irrigation water amounts of maize under different CO_2 concentrations were 528 (400 μmol mol^{-1}), 455 (550 μmol mol^{-1}), 445 (700 μmol mol^{-1}), and 464 (900 μmol mol^{-1}) mm in 2015, and 415 (400 μmol mol^{-1}), 355 (550 μmol mol^{-1}), and 333 (700 μmol mol^{-1}) mm in 2016, respectively. The amount of fertilizer used for each pot was the same. During the growth period each pot was fertilized with 1.5 g urea and 1.5 g diammonium phosphate on five occasions in 2015 and with 0.85 g urea

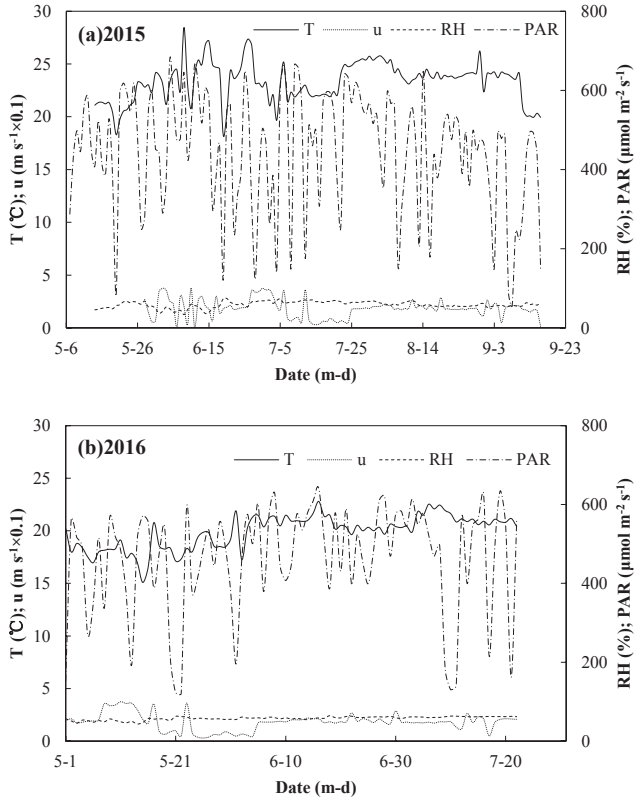

Fig. 1. Variation of daily average temperature (*T*), wind speed (*u*), relative humidity (*RH*), and photosynthetically active radiation (*PAR*) in the phytotron during the growing stage of maize in 2015 and 2016.

and 0.85 g diammonium phosphate on three occasions in 2016. A foliar spray of 250 ml potassium dihydrogen phosphate solution at a concentration of 2% was administered to each plant five times in 2015 and three times in 2016.

2.2. Measurements

2.2.1. Meteorological data and CO_2 concentration

The conventional meteorological data in each chamber, such as photosynthetically active radiation (*PAR*), air temperature (*T*), relative humidity (*RH*), and wind speed (*u*), were monitored and recorded by a portable automatic weather station (HOBO U30, Onset Computer Corp., USA) and a multi-functional automatic anemometer (VELOCICALC 9565, TSI Inc., USA) at 30-minute intervals. The daily average values of meteorological data for the chambers during the experiment are shown in Fig. 1. The CO_2 concentrations were monitored and recorded by the CO_2 gas sensors installed in the chambers at 1-second intervals.

2.2.2. Soil moisture content

Soil moisture content (θ) was measured and recorded by the sensors of portable automatic weather stations (HOBO, S-SMD-M005, Onset Computer Corp., USA). The observed soil moisture content was calibrated using the oven-dried method (ASTM D2216, 1998) before the start of the experiment.

2.2.3. Crop height and leaf area index

After the emergence of the maize, six plants representative of each treatment were randomly selected to measure leaf length, maximum leaf width, and plant height. A steel tape graduated in cm was used and observations were made every seven to ten days. The leaf area of an individual leaf was calculated as leaf length multiplied by the maximum leaf width and then multiplied by a scaling factor of 0.74 (Li et al., 2014). The leaf area index (*LAI*, $m^2\,m^{-2}$) was defined as the ratio of the total leaf area of one plant to the surface area of the soil in the plastic pot.

2.2.4. Evapotranspiration

Evapotranspiration was calculated using the water balance method. Since the maize plants were grown in pots in the chambers, there was no need to consider precipitation, surface runoff, or groundwater supply. A tray was placed below every pot to collect drainage or leakage water, but no drainage or leakage from the pots was observed. Thus, the water balance equation can be simplified to the following:

$$ET = I - \Delta W \tag{1}$$

where *ET* is crop evapotranspiration ($mm\,d^{-1}$), *I* is the irrigation amount ($mm\,d^{-1}$), and ΔW is the difference between two weighings ($mm\,d^{-1}$).

2.2.5. Stomatal conductance

The stomatal conductance of water vapor diffusion (g_s) from the maize leaves was measured using an LI-6400 photosynthesis system (LI-COR Inc., USA). The second leaves of each of six representative plants that were undergoing the same treatment were randomly selected for measurement. The g_s of each selected leaf was recorded at two-hour intervals from 8:00 h to 18:00 h on July 10, July 17, and August 15 in 2015, and June 12, June 15, June 17, June 21, and June 23 in 2016. The maximum g_s (g_{smax}) values of each treatment were used to validate the three different relationships of stomatal conductance and CO_2 concentrations.

2.3. Data collection

Fifty representative journal articles concerning the effect of elevated CO_2 concentration on crop stomatal conductance were selected to collect the g_s data with corresponding CO_2 concentrations. The maximum values of g_s data within each literature were chosen to be g_{smax} with the presumption that the environmental conditions were optimal (i.e. $f(R_n) = f(T) = f(VPD) = f(\theta) = 1$ in the Eq. [4b] described in Section 2.4.2). The articles were published in the years 1971–2016, and the CO_2 concentrations ranged from 100 to 1800 $\mu mol\,mol^{-1}$. Both C_3 and C_4 crops were included in the literature. The experimental environments included growth chambers (GC), greenhouses (GH), open-top chambers (OTC), free-air CO_2 enrichment (FACE) devices, daylight soil–plant–atmosphere research chambers (SPARC), and a new process-based model to capture the crop–weather relationship over a large area (MCWLA model). Information on the works cited from the literature is given in the Appendix.

2.4. Models

2.4.1. Penman–Monteith model

The Penman–Monteith model (P-M) is used to estimate crop evapotranspiration (*ET*) as follows (Monteith, 1965):

$$\lambda ET = \frac{\Delta(R_n - G) + C_p \rho_a VPD / r_a}{\Delta + \gamma[1 + 1/(g_c \cdot r_a)]} \tag{2}$$

where λ is the latent heat of vaporization ($MJ\,kg^{-1}$), *ET* is the crop evapotranspiration ($mm\,d^{-1}$), Δ is the slope of the water vapor saturation pressure versus temperature curve ($kPa\,K^{-1}$), R_n is the net radiation ($W\,m^{-2}$), *G* is the soil heat flux ($W\,m^{-2}$), C_p is the specific heat of dry air at constant pressure ($MJ\,kg^{-1}\,°C^{-1}$), ρ_a is the air density ($kg\,m^{-3}$), *VPD* is the water vapour pressure deficit (kPa), r_a is the aerodynamic resistance ($s\,m^{-1}$), γ is the psychrometric constant ($kPa\,°C^{-1}$), and g_c is the canopy conductance ($m\,s^{-1}$). The following expression can be used to calculate r_a (Thom, 1972):

$$r_a = \frac{\ln((Z-d)/(h_c-d))\ln((Z-d)/Z_o)}{k^2 u_z} \quad (3)$$

where Z is the reference height (m), h_c is the mean crop height (m), d is the zero plane displacement (m) and $d = 0.67h_c$, Z_o is the roughness length of the crop relative to momentum transfer (m) and $Z_o = 0.13h_c$, k is the Karman constant (0.41), and u_z is the wind speed at the reference height ($m\,s^{-1}$).

2.4.2. Jarvis canopy conductance model

The Jarvis canopy conductance model (Jarvis model) can be expressed as (Jarvis, 1976; Stewart, 1988):

$$g_c = g_s \cdot LAI_{active} \quad (4a)$$

where g_s is the leaf stomatal conductance given by:

$$g_s = g_{s\max ref} \cdot f(R_n) \cdot f(T) \cdot f(VPD) \cdot f(\theta) \cdot f(CO_2) \quad (4b)$$

where g_c is the canopy conductance ($m\,s^{-1}$), LAI_{active} is the effective leaf area index ($m^2\,m^{-2}$), $g_{smaxref}$ is the species-dependent maximum leaf stomatal conductance observed in optimal climatic conditions obtaining under the reference CO_2 concentration (0.0061 $m\,s^{-1}$, based on observed data), R_n is the net radiation ($W\,m^{-2}$), T is the air temperature (°C), VPD is the water vapour pressure deficit (kPa), θ is the soil water content ($cm^3\,cm^{-3}$), and CO_2 is the CO_2 concentration ($\mu mol\,mol^{-1}$). The values of the submodels (i.e. $f(R_n)$, $f(T)$, $f(VPD)$, $f(\theta)$, and $f(CO_2)$) are between 0 and 1.

The parameter g_c is related to environmental variables, one of which is the effective leaf area index, which is calculated as (Gardiol et al., 2003; Zhang et al., 2008):

$$LAI_{active} = \begin{cases} LAI & LAI \le 2 \\ 2 & 2 < LAI < 4 \\ 0.5LAI & LAI \ge 4 \end{cases} \quad (5)$$

where LAI is the leaf area index ($m^2\,m^{-2}$).

The net radiation component of the Jarvis model and the parameter f can be expressed as (Tourula and Heikinheimo, 1998):

$$f(R_n) = \frac{g_{s\min}/g_{s\max ref} + f}{1+f} \quad (6)$$

$$f = 0.55\frac{R_n}{LAI} \quad (7)$$

where g_{smin} is the minimum stomatal conductance, which is set to $2 \times 10^{-4}\,m\,s^{-1}$ (Chen and Dudhia, 2001).

The temperature component of the Jarvis model can be expressed as (Dickinson, 1984; Noilhan and Planton, 1989; Lhomme et al., 1998):

$$f(T) = 1 - 0.0016 \times (25 - T)^2 \quad (8)$$

where $0.0016\,°C^{-1}$ is the empirical parameter and 25 °C is the optimum temperature for crop growth (Noilhan and Planton, 1989; Mo, 1997).

The humidity component of the Jarvis model can be expressed as (Jarvis, 1976; Stewart, 1988; Noilhan and Planton, 1989):

$$f(VPD) = 1 - 0.0025 \times VPD \quad (9)$$

where $0.0025\,kPa^{-1}$ is the empirical parameter.

The soil moisture component of the Jarvis model can be expressed as (Noilhan and Planton, 1989; Dolman, 1993):

$$f(\theta) = \begin{cases} 1 & \theta \ge \theta_F \\ \frac{\theta - \theta_W}{\theta_F - \theta_W} & \theta_W < \theta < \theta_F \\ 0 & \theta \le \theta_W \end{cases} \quad (10)$$

where θ is the soil moisture content ($cm^3\,cm^{-3}$), θ_W is the wilting moisture content ($cm^3\,cm^{-3}$), and θ_F is the field capacity ($cm^3\,cm^{-3}$).

2.4.3. Three CO_2-dependent stomatal conductance submodels

The CO_2-dependent quantity g_{smax} is defined by:

$$g_{s\max} = g_{s\max ref} \cdot f(CO_2) \quad (11)$$

where the maximum stomatal conductance g_{smax} is the value of g_s when the environmental variables R_n, T, VPD, and θ are non-limiting (i.e. $f(R_n) = f(T) = f(VPD) = f(\theta) = 1$) to eliminate their effects on g_s and to determine the CO_2-dependent submodel $f(CO_2)$, and $g_{smax}/g_{smaxref} = 1$ when $f(CO_2) = 1$.

There are three different CO_2-dependent stomatal conductance submodels tested in this study. The linear model is expressed as (Easterling et al., 1992; Wu et al., 2012):

$$f(CO_2) = \frac{g_{s\max}}{g_{s\max ref}} = 1 - p\left(\frac{CO_2}{CO_{2ref}} - 1\right) \quad (12)$$

where p is an empirical parameter and indicates the extent to which g_s decreases when the CO_2 concentration is doubled. The p value 0.4 was obtained from a large literature study by Morison (1987). CO_{2ref} is the reference CO_2 concentration, which is set to 330 $\mu mol\,mol^{-1}$.

The hyperbolic model is (Wang et al., 2005; Wang and Wen, 2010):

$$f(CO_2) = \frac{g_{s\max}}{g_{s\max p}} = \frac{1}{1 + \frac{CO_2}{C_{s0}}} \quad (13)$$

where C_{s0} is the empirical parameter ($\mu mol\,mol^{-1}$), and g_{smaxp} is the potential maximum stomatal conductance when using this model. The values $C_{s0} = 305\,\mu mol\,mol^{-1}$ and $g_{smaxp} = 0.018\,m\,s^{-1}$ were obtained from the CO_2 data and the corresponding g_{smax} data of the 50 articles in the Appendix by using the least square method.

Combined the g_s-CO_2 relationship framework from Eq. [12] and hyperbolic relationship from Eq. [13], a modified hyperbolic model was derived by the authors, which is:

$$f(CO_2) = \frac{g_{s\max}}{g_{s\max ref}} = \frac{1}{1 + b\left(\frac{CO_2}{CO_{2ref}} - 1\right)} \quad (14)$$

where b is an empirical parameter. When $CO_2/CO_{2ref} = 1$, $f(CO_2) = 1$. From the CO_2 data and the corresponding g_{smax} data obtained from the works cited in the Appendix, the value of $b = 0.663$ was obtained by the least square method.

2.5. Data analysis

STATISTICA version 8.0 (StatSoft, Inc., Tulsa, Oklahoma) was used to determine the empirical parameters (C_{s0} and g_{smax} in Eq. [13], and b in Eq. [14]) by the g_{smax} data and the corresponding CO_2 from works cited in the Appendix and the nonlinear least square method. The values of the g_{smax} data and the CO_2 concentrations from the maize experiments in 2015 and 2016 were used for parameter validation. SPSS 21 (SPSS 21.0, SPSS Inc., USA) was used to perform the statistical analysis.

2.6. Evaluation of model performance

The performance of each model was evaluated using six indicators: the linear regression coefficient (B), the coefficient of determination (R^2), the root mean square error ($RMSE$), the Nash–Sutcliffe efficiency coefficient (NSE), the fixed affinity index (d), and the Akaike information criterion (AIC) between the observed and estimated values. The larger R^2 is, the smaller $RMSE$ and AIC are, and the closer B, NSE, and d are to 1, the better is the performance of the model (Li et al., 2016; Niu et al., 2013). R^2, $RMSE$, NSE, d and AIC can be expressed as:

$$R^2 = \frac{\left(\sum_{i=1}^{n}(Q_i - \bar{Q})(P_i - \bar{P})\right)^2}{\sum_{i=1}^{n}(Q_i - \bar{Q})^2 \cdot \sum_{i=1}^{n}(P_i - \bar{P})^2} \quad (15)$$

$$RMSE = \sqrt{\frac{1}{n}\sum_{i=1}^{n}(Q_i - P_i)^2} \quad (16)$$

$$NSE = 1 - \frac{\sum_{i=1}^{n}(Q_i - P_i)^2}{\sum_{i=1}^{n}(Q_i - \bar{Q})^2} \quad (17)$$

$$d = 1 - \frac{\sum_{i=1}^{n}|Q_i - P_i|}{\sum_{i=1}^{n}(|Q_i - \bar{Q}| + |P_i - \bar{Q}|)} \quad (18)$$

$$AIC = (-2)\cdot Ln(L) + 2q \quad (19)$$

where Q_i is the observed value, P_i is the estimated value, $\bar{Q}$ is the mean observed value, $\bar{P}$ is the mean estimated value, L is the maximum likelihood function of the model, and q is the number of independent parameters of the model.

3. Results and discussion

3.1. Relationship between stomatal conductance and CO_2 concentration

In the Jarvis canopy conductance model (Eq. [4]), we can see that the g_c was calculated by $g_{smaxref}$ and modified by LAI_{active} and some environmental variables (i.e. R_n, T, VPD, θ, and CO_2). In other words, the submodels are used to modify $g_{smaxref}$. So if we know the $g_{smaxref}$ at the reference CO_2 concentration and the equations of the submodels, we can know exactly the g_c part. Since the environmental variable submodels except CO_2 have been known well (Noilhan and Planton, 1989; Chen and Dudhia, 2001), we would like to look at the relationship between g_{smax} and CO_2 in Eq. [11].

Fig. 2 shows the changes in g_{smax} with the increases in atmospheric CO_2 concentrations as observed in the experiments in 2015 and 2016 and in the works cited in the Appendix. It can be seen from Fig. 2a that g_{smax} as observed in the two-year experiment decreases as the CO_2 concentration increases, and that the reduction rate of g_{smax} (i.e. the slope on the curve) gradually lessens as the CO_2 concentration increases.

In order to supplement the amount of the experimental data and thereby increase the credibility of the research results, we investigated large amount of literatures and carefully selected 50 papers that examined the influence of elevated CO_2 concentration on stomatal conductance. And then we selected 20 of them in which at least three CO_2 concentration gradients were considered for the purpose to exactly draw the g_{smax} and CO_2 trend lines. The changes in g_{smax} with the increases in CO_2 concentrations in these works are shown in Fig. 2b. Fig. 2b shows that all the g_{smax} decreases as the CO_2 concentration increases. The magnitude of g_{smax} varies widely among the cited works, for example, some show very steep decline as CO_2 concentration increases whereas other studies show a much smaller response. However, the most important indication is that the relationship between g_{smax} and CO_2 concentration is not a simple linear one, but that the data are better fitted with a nonlinear curve. This observation is consistent with the early results of Health and Russell (1954), whose study showed a nonlinear response between g_s and CO_2 concentration, Morison and Gifford (1983), who used a quadratic curve to fit the g_s-CO_2 relationship, and Wang and Wen (2010), who used a hyperbolic curve to represent the relationship between g_s and CO_2 concentration.

The widely ranged values of g_{smax} are because of the different crop species (e.g. maize, wheat, sorghum, cotton, rice, barley, sugarcane, soybean, etc.) and the growth conditions (e.g. growth chambers (GC), free-air CO_2 enrichment experiment (FACE), open-top chambers (OTC), etc.). In order to examine these effects on g_{smax}, we plotted the data identifying the crop types and the growth conditions (Fig. 2c and d). It shows that g_{smax} also has widely range in the magnitude and decline trend both for C_3 and C_4 types (Fig. 2c), as well as for GC, FACE, and OTC conditions (Fig. 2d). So it can be concluded that the g_{smax}-CO_2 relationships in absolute values do not specifically and uniformly belong to any crop types or growth conditions, which means there was no clear grouping of the stomatal responses to CO_2 with respect to crop type or treatment.

In the widely recognized theory of malate metabolism (Casati et al., 1999; Reckmann et al., 1990; Shi, 1995; Yu and Wang, 2010), which concerns the mechanism of stomatal movement, photosynthesis changes the CO_2 concentration of mesophyll cells (C_i) and eventually drives stomatal operation. The effect of atmospheric CO_2 concentration on g_s is mainly achieved by changing C_i through influencing photosynthesis (Yu and Wang, 2010). The carbon fixation activity of RuBisCO, one of the key enzymes responsible for photosynthesis, is controlled by C_i and the concentration of oxygen (Genkov et al., 2010; Wang and Wen, 2010). Because the effect of CO_2 concentration on g_s occurs as a biochemical reaction that is controlled by RuBisCO, and because there is a nonlinear relationship between the rate of the biochemical reaction and C_i (Farquhar et al., 1980), the response of g_s to changes in the CO_2 concentration is also nonlinear (Wang and Wen, 2010).

3.2. Calibration and validation of parameters in the three CO_2-dependent stomatal conductance submodels

In order to calibrate and validate submodel parameters, and to eliminate the influence of differences in magnitude in the values of g_{smax} on model parameters, also considering that the inputs and outputs in Eqs. [12]–[14] are relative values, the data obtained from both the cited works and the experiments were converted to relative CO_2 concentrations (CO_2/CO_{2ref}) and relative maximum stomatal conductance ($g_{smax}/g_{smaxref}$), as shown in Fig. 3. Similar to Fig. 2, the relative values were also plotted identifying crop types (C_3 and C_4) and growth conditions (GC, FACE, and OTC) as shown in Fig. 3c and d. It can be seen that for C_3 and C_4 crops, the fitted decline trends (curves) are almost the same one, as well as for GC, FACE, and OTC conditions. Thus, the relationships between $g_{smax}/g_{smaxref}$ and CO_2/CO_{2ref} are not affected by either crop types or growth conditions. Therefore, by applying all the collected data (Fig. 3b) together into the least square method, the values of $C_{s0} = 305\ \mu mol\ mol^{-1}$ and $g_{smaxp} = 0.018\ m\ s^{-1}$ in Eq. [13], and $b = 0.663$ in Eq. [14] were obtained.

The experimental g_{smax} data and CO_2 concentrations, in total 7 sets, that were measured in 2015 and 2016 (Fig. 3a) were used to validate the three submodels. The $g_{smax}/g_{smaxref}$ estimated by the linear model, the hyperbolic model, and the modified hyperbolic model are distinguished as g_{sL}, g_{sH}, and g_{sM}, respectively. These values were compared with the measured relative maximum stomatal conductance (g_{sa}). The results are shown in Table 1.

Table 1 lists the linear regression coefficients (B), the coefficients of determination (R^2), the root mean square errors ($RMSE$), the Nash-Sutcliffe efficiency coefficients (NSE), the fixed affinity indexes (d), and the Akaike information criteria (AIC) values obtained by regression analysis between the observed g_{sa} and the estimated g_{sL}, g_{sH}, and g_{sM}. The table shows that the values of B for the relationships between g_{sL} and g_{sa} and between g_{sM} and g_{sa} (1.02 and 1.00 respectively) are nearly the same, and that the value of B for the relationship between g_{sH} and g_{sa} is the highest with a value of 1.22. Of the other indicators, the values of R^2, NSE, and d (0.97, 0.96, and 0.93, respectively) for the relationship between g_{sM} and g_{sa} are the highest; the values of R^2, NSE, and d (0.65, −0.21, and 0.49, respectively) for the relationship between g_{sH} and g_{sa} are the lowest; and the values of R^2, NSE, and d (0.89, 0.86, and 0.84, respectively) for the relationship between g_{sL} and g_{sa} are intermediate. The values of $RMSE$ and AIC (0.03 and −47.48 respectively) for the relationship between g_{sM} and g_{sa} are the lowest; the values of $RMSE$ and AIC (0.07 and −37.42 respectively) for the relationship between g_{sH} and g_{sa} are the highest; and the values of $RMSE$ and AIC (0.06 and −38.10 respectively) for the relationship between g_{sL} and g_{sa} are intermediate. All these parameters show a consistent result: in the three submodels, the modified hyperbolic model is the most accurate and shows the best fit between estimated and observed data for g_s, followed by the linear model and the hyperbolic model.

Increased CO_2 concentration undoubtedly has an effect on g_s, but

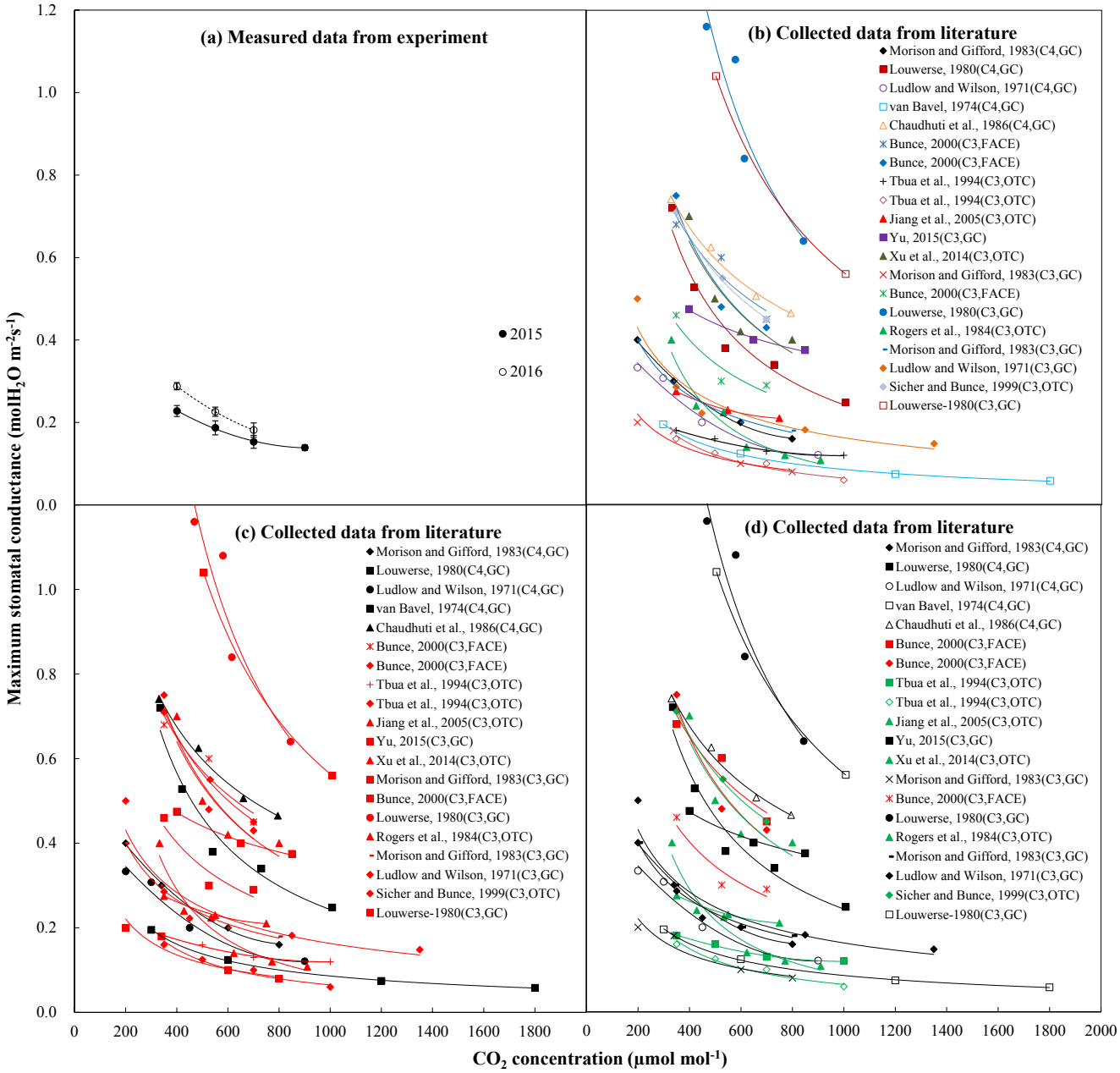

Fig. 2. Maximum stomatal conductance and CO_2 concentration (a) observed in the 2015 and 2016 experiments, (b) selected from the works cited in the Appendix, (c) selected data plotted identifying the different crop types (C_4 in black and C_3 in red), and (d) selected data plotted identifying the different growth conditions (GC in black, FACE in red, and OTC in green). (For interpretation of the references to colour in this figure legend, the reader is referred to the web version of this article.)

scholars disagree in their understanding of the mathematical relationship between the two. Jarvis (1976) thought that g_s decreased linearly with the increase in CO_2 concentration within the range 100–1000 μmol mol^{-1}. Morison and Gifford (1983) used a quadratic function to represent the relationship between g_s and CO_2 concentration within the range 200–800 μmol mol^{-1}. Since Morison (1987) found that doubling the CO_2 concentration would result in a 40% decrease in g_s within the range 330–660 μmol mol^{-1}, Easterling et al. (1992) included that results in a linear model to represent the response of g_s to change in CO_2 concentration in order to estimate the effect of increased CO_2 concentration on *ET*. The results of our study show that the response of g_s to change in CO_2 concentration can be accurately approximated by a linear relationship within a limited range of CO_2 concentrations, and within this range both the linear model and the modified hyperbolic model show a good fit for g_s. However, when the CO_2 concentration is beyond this range, the decrease in g_s gradually lessens as the CO_2 concentration increases, which shows a nonlinear relationship. In this case the linear model will overestimate the effect of increasing CO_2 concentration on g_s.

3.3. Comparison of observed ET and ET estimated by the Penman–Monteith model without stomatal-CO_2 response

The comparison of the observed *ET* (ET_a) and estimated *ET* (ET_R) by P-M model without stomatal-CO_2 response (i.e. $f(CO_2) = 1$) was shown in Table 2 and Fig. 4. In Fig. 4, it shows that the estimated ET_R was not good, it was higher than the observed ET_a when taking no account of the CO_2 concentration effect on g_s, especially under the high CO_2 concentrations (e.g. 550, 700, and 900 μmol mol^{-1}). And the higher the CO_2 concentration, the larger the estimation error was between ET_a and ET_R: the estimation errors were respectively 4% (400 μmol mol^{-1}), 9% (550 μmol mol^{-1}), 10% (700 μmol mol^{-1}), and 8% (900 μmol mol^{-1}).

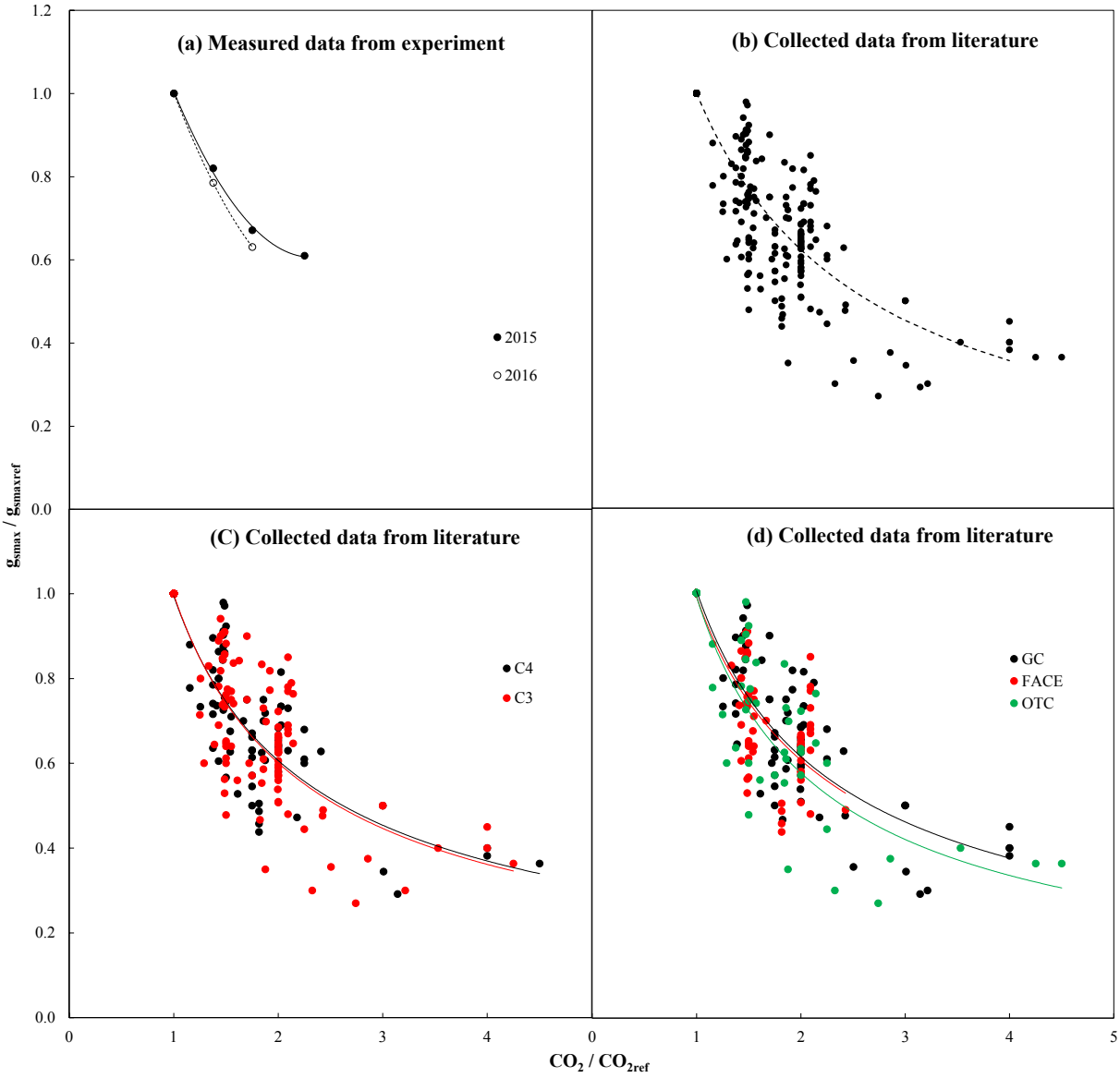

Fig. 3. Relationship between relative maximum stomatal conductance ($g_{smax}/g_{smaxref}$) and relative CO_2 concentration (CO_2/CO_{2ref}) for (a) observed data in the 2015 and 2016 experiments, (b) collected data from the works cited in the Appendix, (c) collected data plotted identifying the different crop types (C_4 in black and C_3 in red), and (d) collected data plotted identifying the different growth conditions (GC in black, FACE in red, and OTC in green). The curves are fitted modified hyperbolic functions. Abbreviations: g_{smax}, CO_2-dependent maximum stomatal conductance; $g_{smaxref}$, maximum stomatal conductance at the reference CO_2 concentration; CO_2, atmospheric CO_2 concentration; CO_{2ref}, reference CO_2 concentration, which is set to 330 μmol mol^{-1}. (For interpretation of the references to colour in this figure legend, the reader is referred to the web version of this article.)

Table 1
Validation of three CO_2-dependent stomatal conductance models using observed maximum stomatal conductance and CO_2 concentration data from the 2015 and 2016 experiments; g_{sa} is the observed relative maximum stomatal conductance; g_{sL}, g_{sH}, and g_{sM} are the estimates of relative maximum stomatal conductance given by the linear model, the hyperbolic model, and the modified hyperbolic model, respectively; R^2 is the coefficient of determination, *RMSE* is the root mean square error, *NSE* is the Nash–Sutcliffe efficiency coefficient, *d* is the fixed affinity index, *AIC* is the Akaike information criterion.

Model	Regression equation	R^2	RMSE	NSE	d	AIC
Linear model	$g_{sL} = 1.02g_{sa}$	0.89	0.06	0.86	0.84	−38.10
Hyperbolic model	$g_{sH} = 1.22g_{sa}$	0.65	0.07	−0.21	0.49	−37.42
Modified hyperbolic model	$g_{sM} = 1.00g_{sa}$	0.97	0.03	0.96	0.93	−47.48

That was because g_s decreases with the elevation of CO_2 concentration, and there is a positive relationship between *ET* and g_s. Without the response of g_s to CO_2 concentration, the ET_R by P-M model would be overestimated when compared with ET_a. And the estimation errors would be more and more obvious along with the elevation of CO_2 concentration when the effect of CO_2 concentration on g_s increases. Therefore, when estimating *ET* by P-M model under elevated CO_2 concentration, it is important and necessary to incorporate the proper g_s-CO_2 submodel to improve the estimation accuracy of *ET*.

3.4. Comparison of observed ET and ET estimated by the Penman–Monteith model using three CO_2-dependent stomatal conductance submodels

From the linear regression coefficients of the relationship between observed *ET* (ET_a) and estimated *ET* using the linear model (ET_L), the hyperbolic model (ET_H), and the modified hyperbolic model (ET_M),

Table 2
Comparative analysis of estimated *ET* using the Penman–Monteith model without stomatal-CO_2 response (ET_R) and in three CO_2-dependent stomatal conductance models (ET_L, the linear model, ET_H, the hyperbolic model, and ET_M, the modified hyperbolic model) and observed *ET* (ET_a); g_s is the stomatal conductance, R^2 is the coefficient of determination, *RMSE* is the root mean square error (mm d^{-1}), *NSE* is the Nash–Sutcliffe efficiency coefficient, *d* is the fixed affinity index, and *AIC* is the Akaike information criterion.

CO_2 (μmol mol^{-1})	Model	Regression equation	R^2	RMSE (mm d^{-1})	NSE	d	AIC
400	Without g_s-CO_2 response	$ET_R = 1.04ET_a$	0.78	0.74	0.81	0.78	−65.17
	Linear model	$ET_L = 1.03ET_a$	0.78	0.71	0.83	0.79	−73.39
	Hyperbolic model	$ET_H = 1.07ET_a$	0.77	0.79	0.78	0.75	−47.13
	Modified hyperbolic model	$ET_M = 1.02ET_a$	0.78	0.70	0.83	0.79	−75.84
550	Without g_s-CO_2 response	$ET_R = 1.09ET_a$	0.78	0.68	0.76	0.75	−82.13
	Linear model	$ET_L = 1.05ET_a$	0.80	0.59	0.83	0.78	−116.81
	Hyperbolic model	$ET_H = 1.08ET_a$	0.78	0.67	0.77	0.75	−85.97
	Modified hyperbolic model	$ET_M = 1.04ET_a$	0.80	0.58	0.83	0.78	−119.27
700	Without g_s-CO_2 response	$ET_R = 1.10ET_a$	0.81	0.62	0.77	0.76	−104.85
	Linear model	$ET_L = 0.99ET_a$	0.83	0.48	0.86	0.82	−163.26
	Hyperbolic model	$ET_H = 1.06ET_a$	0.82	0.54	0.82	0.79	−131.82
	Modified hyperbolic model	$ET_M = 1.01ET_a$	0.83	0.48	0.86	0.82	−162.48
900	Without g_s-CO_2 response	$ET_R = 1.08ET_a$	0.73	0.63	0.77	0.73	−59.25
	Linear model	$ET_L = 0.90ET_a$	0.72	0.63	0.77	0.73	−59.57
	Hyperbolic model	$ET_H = 1.03ET_a$	0.75	0.51	0.85	0.78	−85.82
	Modified hyperbolic model	$ET_M = 0.99ET_a$	0.76	0.47	0.88	0.81	−98.68

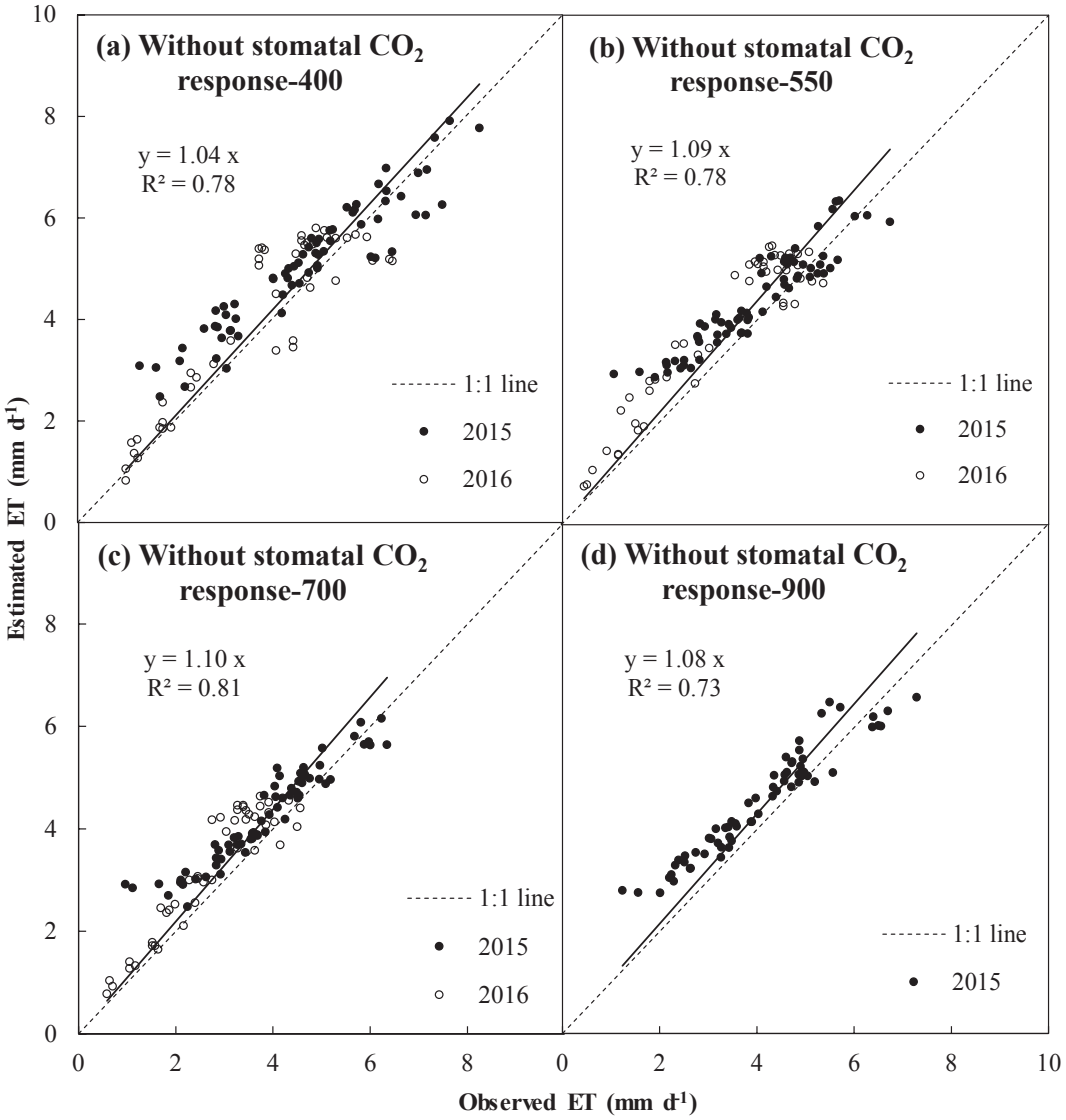

Fig. 4. The linear relationship of estimated *ET* by Penman-Monteith model without stomatal CO_2 response and the observed *ET* obtained by the water balance method.

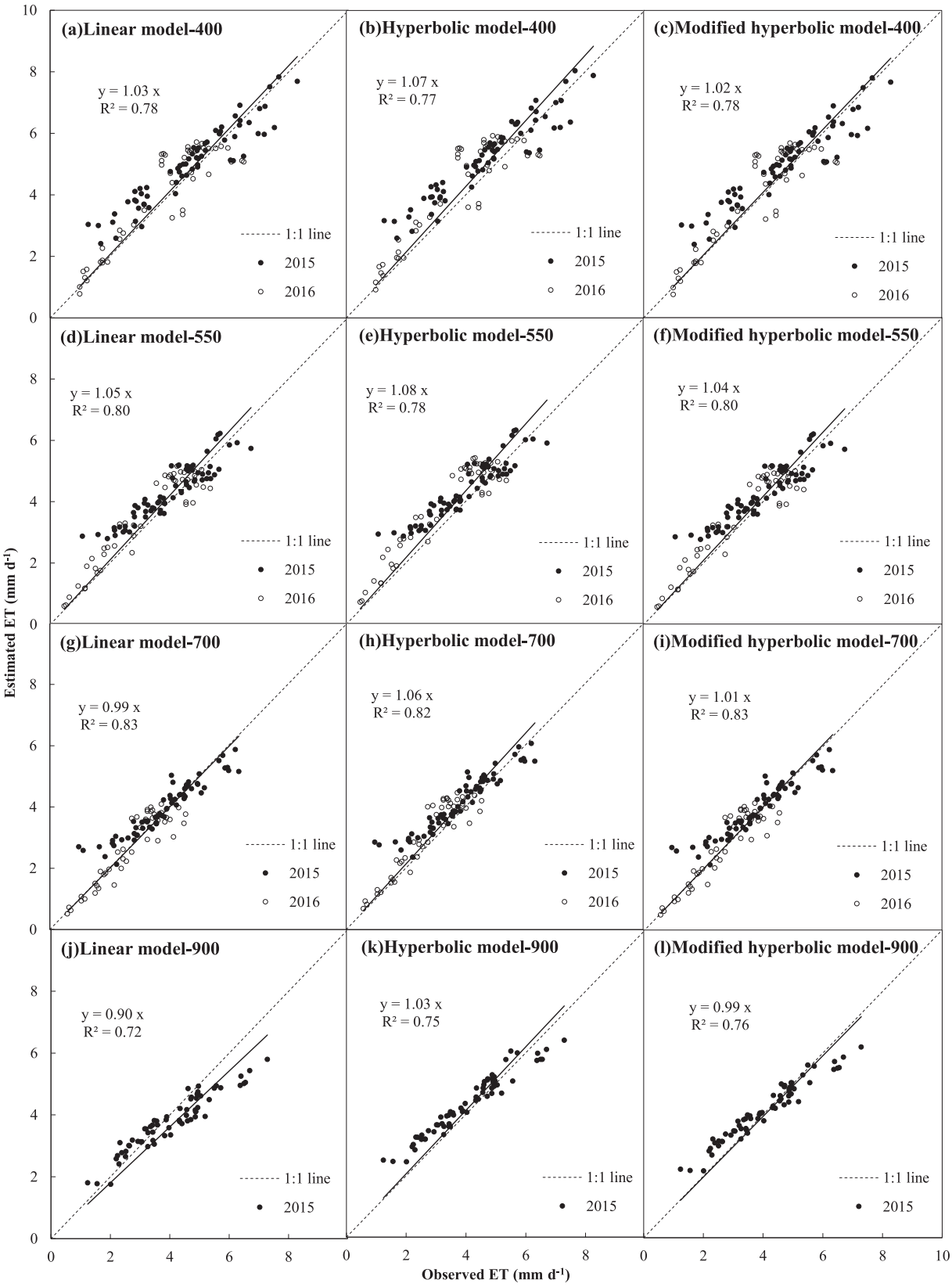

Fig. 5. Comparison of daily average *ET* estimated by the Penman–Monteith model using three CO_2-dependent stomatal conductance submodels (the linear model, the hyperbolic model, and the modified hyperbolic model) with the observed *ET* obtained by the water balance method.

which are shown in Table 2 and Fig. 5, it can be seen that the hyperbolic model overestimated *ET* for all four CO_2 concentrations (Fig. 5b, e, h, and k). When the CO_2 concentration was no more than 550 μmol mol^{-1}, ET_H and ET_R had similar estimation results with the close values of R^2, *RMSE*, *NSE*, *d*, and *AIC*. When the CO_2 concentration was higher than 550 μmol mol^{-1}, the accuracy of ET_H by the hyperbolic model was improved when compared with ET_R which was estimated without the CO_2 concentration effect. And all the above five evaluation parameters of ET_H had an advantage over that of ET_R (Table 2).

In Table 2, it shows that the estimation accuracies of *ET* by linear model and modified hyperbolic model were higher than that by hyperbolic model and without CO_2 concentration effect. When the CO_2 concentration was 400 and 550 μmol mol^{-1}, ET_L and ET_M also overestimated ET_a to some degree: the estimation errors were respectively 2.5% and 1.9% (400 μmol mol^{-1}) and 4.7% and 4.3% (550 μmol mol^{-1}), but all better than ET_H and ET_R. When the CO_2 concentration was 700 μmol mol^{-1}, ET_L and ET_M gave reasonably accurate estimates of ET_a, with errors of 0.6% and 0.9%, respectively. When the CO_2 concentration was 900 μmol mol^{-1}, ET_L significantly underestimated ET_a, while ET_M gave a reasonably accurate estimate of ET_a, with errors of 9.7% and 1.4%, respectively.

When the CO_2 concentration was less than 900 μmol mol^{-1}, although ET_L and ET_M were more accurate in estimating ET_a, the values of R^2, *NSE*, and *d* for the relationship between ET_M and ET_a were larger than those for the relationship between ET_L and ET_a, and the values of *RMSE* and *AIC* for the relationship between ET_M and ET_a were smaller than those for the relationship between ET_L and ET_a. The evaluation indicators (R^2, *RMSE*, *NSE*, *d*, and *AIC*) for the relationship between ET_R and ET_a, as well as ET_H and ET_a were the worst (Table 2). Thus, the modified hyperbolic model gave the best estimation of ET_a. When the CO_2 concentration was 900 μmol mol^{-1}, ET_L gave the worst estimate of ET_a, and the evaluation indicators showed the worst performance, which was similar with that of ET_R. The models of ET_H and ET_M gave better estimates of ET_a, but the values of R^2, *NSE*, and *d* for the relationship between ET_M and ET_a were the largest, and the values of *RMSE* and *AIC* were the smallest. Thus the modified hyperbolic model was still the best model and gave the most accurate estimate of *ET* when the CO_2 concentration was higher.

Because the exact fitting of g_s played an important role in the estimation of *ET* by P-M, the hyperbolic model performed consistently worse in the estimation of g_s and *ET* than either the linear model or the modified hyperbolic model. The hyperbolic model only considered the relationship between the absolute CO_2 concentration and the absolute g_s which is highly dependent on crop species; the potential maximum g_s (g_{smaxp}) and the parameter C_{s0} in Eq. [13] were empirical values which were highly dependent on the original data, namely if the calibration data set changed, the g_{smaxp} and C_{s0} would also like to change. The g_s values found in the different literature sources were often quite different, which can significantly influence the calibration process for g_{smaxp} and C_{s0}. Thus, the hyperbolic model may not be suitable for *ET* estimation by P-M if atmospheric CO_2 concentration increases.

In order to eliminate the influence of the absolute g_s value on the accuracy of the model, the concepts of relative g_{smax} ($g_{smax}/g_{smaxref}$) and relative CO_2 concentration (CO_2/CO_{2ref}) were introduced into the original hyperbolic model in a way that was consistent with the parameters of the linear model. A comparison between Figs. 3b and 2b also shows that the introduction of the relative values can improve the response of g_s to the decreased impact of higher CO_2 concentration, with more concentrated data points and more stable calibrated empirical parameters in the model. Those who using the model only need to set the reference CO_2 concentration which is already known and a value of maximum stomatal conductance which is species-dependent at the specific CO_2 concentration in order to accurately simulate *ET*. Since other empirical parameters are stable, the modified hyperbolic model has simplified the g_s-CO_2 model, and is easier to be applied.

When $CO_2/CO_{2ref} \leq 2$, the linear model and the modified hyperbolic model both gave basically the same estimate of *ET* (Table 2 and Fig. 5). Therefore, the response of g_s to CO_2 concentration was approximated as a linear relationship when $CO_2/CO_{2ref} \leq 2$. This verified the g_s-CO_2 linear pattern applied in the study of Easterling et al. (1992) in which the response of g_s to CO_2 concentration was linear in an absolute range of 330–660 μmol mol^{-1}. However, Jarvis (1976) overestimated the CO_2 concentration range for this linear response. In our paper we have overcome the limitation of the absolute range by considering that the approximate linear response of g_s to CO_2 concentration will occur within a relative range, i.e. $CO_2/CO_{2ref} \leq 2$. In this situation, the estimates of *ET* by the linear model and by the modified hyperbolic model were close to one another, but the modified hyperbolic model was more accurate and the estimate was better. When $CO_2/CO_{2ref} > 2$, the linear model overestimated the effect of increased CO_2 concentration on g_s, especially at 900 μmol mol^{-1} ($CO_2/CO_{2ref} = 2.727$) when the value of ET_L was much less than that of ET_a, but the accuracy of ET_M was much better than that of ET_L. These results illustrate that the modified hyperbolic model can better estimate the effect of increased CO_2 concentration on g_s. The results are consistent with that of Section 3.2.

Based on the comprehensive analysis of the three different g_s-CO_2 submodels, it is found that when incorporating these models into P-M to estimate *ET* under increased CO_2 concentrations, the factor having most impact on the estimate of *ET* was not the absolute CO_2 concentration level, but the relative CO_2 concentration level, which provides a more accurate estimate of *ET*. When the relative CO_2 concentration ≤ 2.12 (i.e. $\leq$ 700 μmol mol^{-1}), the linear model and the modified hyperbolic model showed no significant difference in *ET* estimation. But when the relative CO_2 concentration > 2.12, using the modified hyperbolic model in P-M can give a more precise and accurate result, and it performs good at all CO_2 concentration levels in this research.

Since the highest CO_2 concentration in our research is 900 μmol mol^{-1}, the modified model is applicable within this range. Because the predicted CO_2 concentration is 936 μmol mol^{-1} under RCP8.5 climate change scenario and 900 μmol mol^{-1} is within this range, the modified model is applicable under all the projected climate change scenarios in estimation of ET and other hydrologic variables.

3.5. Sensitivity analysis of the Penman–Monteith model to different parameters for estimating evapotranspiration

In order to analyze the sensitivity of P-M to the empirical parameters in the three g_s-CO_2 submodels when estimating *ET*, the parameters were changed by ± 40 and ± 20%, and then the percentage change in predicted *ET* was calculated. The results are shown in Table 3, which shows that *ET* increased as *p* and *b* decreased and g_{smaxp} and C_{s0} increased; and that *ET* decreased as *p* and *b* increased and g_{smaxp} and C_{s0} decreased. P-M showed different sensitivities to the different empirical parameters for the *ET* estimation. Change in the parameter *b*

Table 3
Percentage changes in estimated *ET* using the Penman–Monteith model when the fitted parameter values of *p* (in the linear model), g_{smaxp} and C_{s0} (in the hyperbolic model), and *b* (in the modified hyperbolic model) change by ± 40% and ± 20%, respectively.

Year	Parameter	Percentage change			
		−40%	−20%	+20%	+40%
2015	*p*	4.08%	2.43%	−4.18%	−15.42%
	g_{smaxp}	−7.01%	−2.79%	1.98%	3.46%
	C_{s0}	−4.73%	−1.85%	1.33%	2.23%
	b	1.87%	0.92%	−0.89%	−1.75%
2016	*p*	4.23%	2.26%	−2.64%	−5.80%
	g_{smaxp}	−13.48%	−5.61%	4.22%	7.52%
	C_{s0}	−9.07%	−3.65%	2.63%	4.63%
	b	3.22%	1.57%	−1.50%	−2.94%

in the modified hyperbolic model had the least influence on *ET*. When values of *b* were changed by −40, −20, +20, and +40%, *ET* changed only by 1.87, 0.92, −0.89, and −1.75% (2015), and 3.22, 1.57, −1.50, and −2.94% (2016). The influences of the other parameters on *ET* are greater as their percentages change.

The sensitivity analysis results in Table 3 show that changes in the empirical parameters of the linear model and the hyperbolic model had greater influence on *ET*, and the changes in the estimate values had increased uncertainty as the empirical parameters changed. When the modified hyperbolic model was incorporated into P-M to estimate *ET* under increased CO_2 concentrations, changes in the empirical parameter *b* had little influence on estimated *ET*, showing this to be the most stable model and that it had wide applicability.

In this paper, the *p* value (0.4) was selected because it was the most commonly used value in the literature that we analyzed. Using this value, when the CO_2 concentration doubled, g_s decreased by 40%. This value of *p* has been used by most scholars and is applied in different scientific research (Easterling et al., 1992; Neitsch et al. 2005; Niu et al., 2013; Wu et al., 2012). Zheng and Peng (2001) analyzed a large quantity of research and derived a *p* value of 0.3, but this value has not been adopted by other scholars. The use of g_s data from different literature sources, different amounts, and different crops would result in different calibration values of *b*, g_{smaxp}, and C_{s0}. In this paper we comprehensively analyzed a large number of papers, published over a long time period, which included data for most C_3 and C_4 crops; CO_2 concentrations ranged from 100 to 1800 μmol mol^{-1}; and the experimental environment involved open and closed equipment, and pot and field experiments. In this case, the calibrated value of *b* provides a good fit for the nonlinear relationship between g_s and the CO_2 concentration, and thus provide a better estimate of *ET* using P-M. The results are broadly representative and widely applicable. The modified model provides an easier way to estimate *ET* when CO_2 concentration increases in the future. And our work also filled the gap where there is no validation of *ET* estimated by P-M model involving the stomatal-CO_2 relationship.

But there are still some limitations in our research: we only used pot experiment data to validate the parameters and models. However, we thought they are broadly applicable because the parameters in the models were calibrated using the data from many literatures which included both pot and field experiment data. But further validation researches with field experiment data are also needed in the future.

Carbon dioxide enrichment can affect not only stomatal conductance, but also crop growth, for example leaf area index (*LAI*) and crop height (*H*). We already have considered that in our study. The only thing is the *LAI* and *H* data were measured in the experiment, but not simulated using *LAI*/*H*-CO_2 models. That was because we only have the *LAI*/*H* data from our experiment, but don't have the *LAI*/*H* data from the literatures which is hard to collect from the beginning to the end of the growth period and most literatures don't provide all the data. But we will consider improving the *LAI*/*H*-CO_2 model in our future's research.

Another limitation of our work is that we only validated the models for C_4 crop which was planted in growth chambers, but not for C_3 crop or other crops that grown in the field. We will conduct such experiments in the future to improve our work.

4. Conclusions

In this paper, the g_s and CO_2 concentration data obtained from the two-year maize experiment and 50 published papers were analyzed. The results that g_s decreased and that the reduction rate gradually lessened as CO_2 concentration increased were obtained. By comparing the estimated g_s and *ET* from the three g_s-CO_2 models (the linear model, the hyperbolic model, and the modified hyperbolic model) with the observed data, it can be concluded that the modified hyperbolic model provides the best estimates both in g_s and *ET* under all levels of CO_2 concentrations, with the largest values of R^2, *NSE*, and *d*, and the smallest values of *RMSE* and *AIC*, followed in decreasing level of accuracy by the linear model and the hyperbolic model. Furthermore, the modified hyperbolic model was more stable and reliable with the smallest changes in estimated *ET* (< 3%) when the empirical parameters changed ± 40 and ± 20%. Therefore, when estimating *ET* with P-M for increased atmospheric CO_2 concentrations, the inclusion of the modified hyperbolic g_s-CO_2 submodel not only recognizes resultant changes in stomata physiological responses, but also makes the estimate more accurate, more reliable, and more widely representative, and thus gives it greater applicability.

Declaration of interests

None.

Acknowledgements

We greatly appreciate the careful reviews and valuable comments by the anonymous reviewers and the editors, which improved the manuscript. This work is financially supported by the National Natural Science Foundation of China (51621061, 51790534), the Discipline Innovative Engineering Plan (111 Program, B14002), and the Ministry of Water Resources of China (201327).

Appendix

Details of the 50 representative literature citations on the effect of elevated CO_2 concentration on crop stomatal conductance. GC: Growth chamber; GH: Greenhouse; OTC: Open-top chamber; FACE: Free-air CO_2 enrichment; SPARC: Daylit soil–plant–atmosphere research chambers; MCWLA model: a new process-based model to capture the crop–weather relationship over a large area.

Types	Crops	CO_2 (μmol mol^{-1})	Condition	Reference
C_3/C_4	sorghum/vigna luteola	200–900	GC	(Ludlow and Wilson, 1971)
C_4	sorghum	100–1800	GC	(van Bavel, 1974)
C_3/C_4	maize/barley/sunflower	335–1007.5	GC	(Louwerse, 1980)
C_3/C_4	maize/rice/phalaris	200–800	GC	(Morison and Gifford, 1983)
C_3/C_4	wheat/barley/sunflower /oilseed	340–680	GH	(Morison, 1998)
C_3	soybeans	332–910	OTC	(Rogers et al., 1984)
C_3	wheat	340–1200	OTC	(Havelka et al., 1984)
C_3	soybeans	330–800	GC	(Jones et al., 1985)
C_4	sorghum	330–795	GC	(Chaudhuri et al., 1986)
C_3/C_4	maize/sorghum/wheat/barley/soybeans/ cotton/rice	325–680	literature survey	(Cure and Acock, 1986)
C_3	cotton	340–640	OTC	(Idso et al., 1987)

C_3/C_4	maize/wheat/soybeans/barley/cotton	370–550	FACE/OTC	(Hileman et al., 1994; Grossman-Clarke et al., 1999; Leakey et al., 2004, 2006; Sun et al., 2009; Wall et al., 2011)
C_3	wheat	350–1000	OTC	(Tuba et al., 1994)
C_4	maize/sorghum/Sugarcane/grain amaranth	380–690	GH	(Ziska and Bunce, 1997)
C_4	maize	350–1100	GH	(Maroco et al., 1999)
C_3/C_4	C_3/C_4	350–650	literature survey	(Wand et al., 1999)
C_3/C_4	maize/sorghum/wheat/barley/soybeans/potato/cotton	350–700	OTC/GC	(Sicher and Bunce, 1999; Wilson et al., 1999; Bunce, 2000, 2001; Li et al., 2003)
C_4	sorghum	370–570	FACE	(Wall et al., 2001)
C_3	soybeans	350–850	literature survey	(Ainsworth et al., 2002)
C_4	lolium perenne	360–600	FACE	(Ainsworth et al., 2003)
C_3	wheat	350–750	OTC	(Jiang et al., 2005; Fan, 2008)
C_3/C_4	crop/grass	366–567	FACE	(Ainsworth and Rogers, 2007)
C_4	sugarcane	360–720	GH	(Vu and Allen, 2009)
C_4	maize	370–750	MCWLA model	(Tao et al., 2009)
C_4	maize	400–700	GH	(Hladnik et al., 2009)
C_4	maize/millet	390–550	FACE/OTC	(Hao et al., 2010; Meng et al., 2014)
C_3/C_4	maize/rice/sunflower	380–700	OTC	(Vanaja et al., 2011)
C_4	maize	385–550	FACE	(Markelz et al., 2011)
C_4	maize	400–550	OTC	(Silva et al., 2012)
C_3/C_4	maize/soybeans	375–550	FACE	(Bernacchi et al., 2006)
C_3/C_4	maize/soybeans	390–585	FACE	(Ruiz-Vera et al., 2013, 2015)
C_3	wheat	396–760	GC	(Liu et al., 2013)
C_3	wheat	375–500	FACE	(Xie, 2013)
C_3	wheat/potato	400–800	SPARC/OTC	(Fleisher et al., 2014; Xu et al., 2014)
C_3	wheat	400–850	GC	(Yu, 2015)
C_4	maize	400–750	SPARC	(Wijewardana et al., 2016)
C_3	barley	380–550	GC	(Schmid et al., 2016)

References

Ainsworth, E.A., Davey, P.A., Bernacchi, C.J., Dermody, O.C., Heaton, E.A., Moore, D.J., Morgan, P.B., Naidu, S.L., Yoora, H.S., Zhu, X.G., Curtis, P.S., Long, S.P., 2002. A meta-analysis of elevated CO_2 effects on soybean (*Glycine max*) physiology, growth and yield. Global Change Biol. 8, 695–709.

Ainsworth, E.A., Davey, P.A., Hymus, G.J., Osborne, C.P., Rogers, A., Blum, H., Nosberger, J., Long, S.P., 2003. Is stimulation of leaf photosynthesis by elevated carbon dioxide concentration maintained in the long term? A test with *Lolium perenne* grown for 10 years at two nitrogen fertilization levels under Free Air CO_2 Enrichment (FACE). Plant, Cell Environ. 26, 705–714.

Ainsworth, E.A., Rogers, A., 2007. The response of photosynthesis and stomatal conductance to rising [CO_2]: mechanisms and environmental interactions. Plant Cell Environ. 30, 258–270.

Allen, R.G., Pereira, L.S., Raes, D., Smith, M., 1998. Crop Evapotranspiration (Guidelines for Computing Crop Water Requirements) Irrigation and Drainage Paper 56. FAO, Food and Agriculture Organization of the United Nations, Rome, Italy.

Arnold, J.G., Srinivasan, R., Muttiah, R.S., Williams, J.R., 1998. Large area hydrologic modeling and assessment Part I: model development. J. Am. Water Resour. Assoc. 34 (1), 73–89.

ASTM D2216, 1998. Standard Test Method for Laboratory Determination of Water (Moisture) Content of Soil and Rock by Mass. American Society for Testing and Materials, Philadelphia, pp. 5.

Ball, J.T., Woodrow, I.E., Berry, J., 1987. A model predicting stomatal conductance and its contribution to the control of photosynthesis under different environmental conditions. In: Biggins I. Progress in Photosynthesis Research. Martinus Nijhoff Publishers, Netherlands, pp. 221–224.

Bastiaanssen, W.G.M., Noordman, E.J.M., Pelgrum, H., Davids, G., Thoreson, B.P., Allen, R.G., 2005. SEBAL model with remotely sensed data to improve water resources management under actual field conditions. J. Irrig. Drain. Eng. 131 (1), 85–93.

Bernacchi, C.J., Leakey, A.D.B., Heady, L.E., Morgan, P.B., Dohleman, F.G., Mcgrath, J.M., Gillespie, K.M., Wittig, V.E., Rogers, A., Long, S.P., Ort, D.R., 2006. Hourly and seasonal variation in photosynthesis and stomatal conductance of soybean grown at future CO_2 and ozone concentrations for 3 years under fully open-air field conditions. Plant Cell Environ. 29 (11), 2077–2090.

Bunce, J.A., 2000. Responses of stomatal conductance to light, humidity and temperature in winter wheat and barley grown at three concentrations of carbon dioxide in the field. Global Change Biol. 6, 371–382.

Bunce, J.A., 2001. Direct and acclamatory responses of stomatal conductance to elevated carbon dioxide in four herbaceous crop species in the field. Global Change Biol. 7, 323–331.

Casati, P., Drincovich, M.F., Edwards, G.E., Andreo, C.S., 1999. Malate metabolism by NADP-malic enzyme in plant defense. Photosynth. Res. 61 (2), 99–105.

Chaudhuri, U.N., Burnett, R.B., Kirkham, M.B., Kanemasu, E.T., 1986. Effect of carbon dioxide on sorghum yield, root growth, and water use. Agric. For. Meteorol. 37 (2), 109–122.

Chen, F., Dudhia, J., 2001. Coupling an advanced land surface- hydrology model with the penn state-NCAR MM5 modelling system. Part I: model implementation and sensitivity. Mon. Weather Rev. 129, 569–585.

Collatz, G.J., Ball, J.T., Grivet, C., Berry, J.A., 1991. Physiological and environmental regulation of stomatal conductance, photosynthesis and transpiration: a model that includes a laminar boundary layer. Agric. For. Meteorol. 54, 107–136.

Cure, J.D., Acock, B., 1986. Crop responses to carbon dioxide doubling: a literature survey. Agric. For. Meteorol. 38 (1), 127–145.

Dickinson, R.E., 1984. Modeling Evapotranspiration for Three-Dimensional Global Climate Models. In: Hansen, J.E., Takahashi, T. (Eds.), Climate Processes and Climate Sensitivity. American Geophysical Union, Washington, D.C., pp. 58–72.

Dolman, A.J., 1993. A multiple-source land surface energy balance model for use in general circulation models. Agric. For. Meteorol. 65 (1–2), 21–45.

Easterling, W.E., Rosenburg, N.J., McKenney, M.S., Jones, C.A., Dyke, P.T., Williams, J.R., 1992. Preparing the erosion productivity impact calculator (EPIC) model to simulate crop response to climate change and the direct effect of CO_2. Agric. For. Meteorol. 59, 17–34.

Fan, L.L., 2008. The Study of Growth, Physiology, Yield and Quality of the Wheat Responses to Increasing CO_2 Concentration in Different Nitrogen Level. Dissertation for the Master Degree. Anhui Agricultural University, Anhui, pp. 96.

Farquhar, G.D., von Caemmerer, S., Berry, J., 1980. A biochemical model of photosynthesis CO_2 assimilation in leaves of C_3 species. Planta 149 (1), 78–90.

Fleisher, D.H., Barnaby, J., Sicher, R., Resop, J.P., Timlin, D.J., Reddy, V.R., 2014. Potato gas exchange response to drought cycles under elevated carbon dioxide. Agron. J. 106 (6), 2024–2034.

Gardiol, J.M., Serio, L.A., Maggiora, A.I.D., 2003. Modelling evapotranspiration of corn (Zea mays) under different plant densities. J. Hydrol. 217, 188–196.

Genkov, T., Meyer, M., Griffiths, H., Spreitzer, R.J., 2010. Functional hybrid rubisco enzymes with plant small subunits and algal large subunits: engineered rbcS cDNA for expression in chlamydomonas. J. Biol. Chem. 285 (26), 19833–19841.

Grossman-Clarke, S., Kimball, B.A., Hunsaker, D.J., Long, S.P., Garcia, R.L., Kartschall, Th., Wall, G.W., Printer, P.J., Wechsung, F., LaMorte, R.L., 1999. Effects of elevated atmospheric CO_2 on canopy transpiration in senescent spring wheat. Agric. For. Meteorol. 93 (98), 95–109.

Hao, X.Y., Li, P., Lin, E.D., Tong, C.F., Wei, Q., Wu, G.D., Dong, X.G., 2010. Effects of air CO_2 enrichment on growth and photosynthetic physiology of millet. J. Nucl. Agric. Sci. 24 (3), 589–593 (in Chinese with English abstract).

Havelka, U.D., Wittenbach, V.A., Boyle, M.G., 1984. CO_2-enrichment effects on wheat yield and physiology. Crop Sci. 24 (6), 1163–1168.

Health, O.V.S., Russell, J., 1954. Studies in stomatal behavior. VI. An investigation of the light responses of wheat stomata with the attempted elimination of control by the mesophyll. Part II. Interactions with external carbon dioxide, and general discussion. J. Exp. Bot. 5, 269–292.

Hileman, D.R., Huluka, G., Kenjige, P.K., Sinha, N., Bhattacharya, N.C., Biswas, P.K., Lewin, K.F., Nagy, J., Hendrey, G.R., 1994. Canopy photosynthesis and transpiration of field-grown cotton exposed to free-air CO_2 enrichment (FACE) and differential irrigation. Agric. For. Meteorol. 70, 189–207.

Hladnik, J., Eler, K., Kržan, K., Pintar, M., Vodnik, D., 2009. Short-term dynamics of stomatal response to sudden increase in CO_2 concentration in maize supplied with different amounts of water. Photosynthetica 47 (3), 422–428.

Idso, S.B., Kimball, B.A., Mauney, J.R., 1987. Atmospheric carbon dioxide enrichment

effects on cotton midday foliage temperature: implications for plant water use and crop yield. Agron. J. 79 (4), 667–672.
IPCC, 2013. Climate Change 2013: the physical science basis. Contribution of working group I to the fifth assessment report of the intergovernmental panel on climate change. Cambridge University Press, Cambridge, United Kingdom and New York, NY, USA, pp. 1535.
Jarvis, P.G., 1976. The interpretation of the variations in leaf water potential and stomatal conductance found in canopies in the field. Philos. Trans. R. Soc. B: Biol. Sci. 273, 593–610.
Jiang, X.L., Kang, S.Z., Tong, L., Li, F.S., 2016. Modification of evapotranspiration model based on effective resistance to estimate evapotranspiration of maize for seed production in an arid region of northwest China. J. Hydrol. 538, 194–207.
Jiang, Y.L., Zhang, Q.G., Zhang, S.D., Wang, G.M., Yue, W., Yao, Y.G., 2005. Responses of photosynthetic characteristics, stomatal conductance and transpiration of wheat to the increase of atmospheric CO_2 concentration. J. Anhui Agric. Univ. 32 (2), 169–173 (in Chinese with English abstrct).
Jones, P., Allen, L.H., Jones, J.W., Valle, R., 1985. Photosynthesis and transpiration responses of soybean canopies to short-and long-term CO_2 treatments. Agron. J. 77, 119–126.
Kang, S.Z., Zhang, F.C., Hu, X.T., Zhang, J.H., 2002. Benefits of CO_2 enrichment on crop plants are modified by soil water status. Plant Soil. 238, 69–77.
Kang, S.Z., Gu, B.J., Du, T.S., Zhang, J.H., 2003. Crop coefficient and ratio of transpiration to evapotranspiration of winter wheat and maize in a semi-humid region. Agric. Water Manage. 59, 239–254.
Leakey, A.D.B., Bernacchi, C.J., Dohleman, F.G., Ort, D.R., Long, S.P., 2004. Will photosynthesis of maize (Zea mays) in the US Corn Belt increase in future [CO_2] rich atmospheres? An analysis of diurnal courses of CO_2 uptake under free-air concentration enrichment (FACE). Global Change Biol. 10, 951–962.
Leakey, A.D.B., Uribelarrea, M., Ainsworth, E.A., Naidu, S.L., Rogers, A., Ort, D.R., Long, S.P., 2006. Photosynthesis, productivity, and yield of maize are not affected by open-air elevation of CO_2 concentration in the absence of drought. Plant Physiol. 140, 779–790.
Lhomme, J.P., Elguero, E., Chehbouni, A., Boulet, G., 1998. Stomatal control of transpiration: examination of Monteith's formulation of canopy resistance. Water Resour. Res. 34 (9), 2301–2308.
Li, S.E., Hao, X.M., Du, T.S., Tong, L., Zhang, J.H., Kang, S.Z., 2014. A coupled surface resistance model to estimate crop evapotranspiration in arid region of northwest China. Hydrol. Processes 28 (4), 2312–2323.
Li, F.S., Kang, S.Z., Zhang, F.C., 2003. Effects of CO_2 concentration, nitrogen and soil moisture on photosynthesis, evapotranspiration and water use efficiency in spring wheat. Chin. J. Appl. Ecol. 14 (3), 387–393 (in Chinese with English abstract).
Li, X.J., Kang, S.Z., Li, F.S., Jiang, X.L., Tong, L., Ding, R.S., Li, S.E., Du, T.S., 2016. Applying segmented Jarvis canopy resistance into Penman-Monteith model improves the accuracy of estimated evapotranspiration in maize for seed production with film-mulching in arid area. Agric. Water Manage. 178, 314–324.
Li, X.J., Kang, S.Z., Zhang, X.T., Li, F.S., Lu, H.N., 2018. Deficit irrigation provokes more pronounced responses of maize photosynthesis and water productivity to elevated CO_2. Agric. Water Manage. 195, 71–83.
Liang, X., Lettenmaier, D.P., Wood, E.F., Burges, S.J., 1994. A simple hydrologically based model of land surface water and energy fluxes for general circulation models. J. Geophys. Res. 99 (D7), 14415–14428.
Liang, X., Lettenmaier, D.P., Wood, E.F., 1996. One-dimensional statistical dynamic representation of subgrid spatial variability of precipitation in the two-layer variable infiltration capacity model. J. Geophys. Res. 101 (D16), 21403–21422.
Liu, Y.Y., Liu, H.L., Qiao, Y.Z., Shi, C.H., Dong, B.D., Li, D.X., Si, F.Y., Jiang, J.W., Zhai, H.M., Liu, M.Y., 2013. Effects of elevated CO_2 concentration and different water conditions on winter wheat growth and water use. Chin. J. Eco. Agric. 21 (11), 1365–1370 (in Chinese with English abstract).
Louwerse, W., 1980. Effects of CO_2 concentration and irradiance on the stomatal behaviour of maize, barley and sunflower plants in the field. Plant Cell Environ. 3, 391–398.
Ludlow, M.M., Wilson, G.L., 1971. Photosynthesis of tropical pasture plants I. Illuminance, carbon dioxide concentration, leaf temperature, and leaf-air vapour pressure difference. Aust. J. Biol. Sci. 24 (3), 449–470.
Markelz, R.J., Strellner, R.S., Leakey, A.D.B., 2011. Impairment of C_4 photosynthesis by drought is exacerbated by limiting nitrogen and ameliorated by elevated [CO_2] in maize. J. Exp. Bot. 62 (9), 3235–3246.
Maroco, J.P., Edwards, G.E., Ku, M.S.B., 1999. Photosynthetic acclimation of maize to growth under elevated levels of carbon dioxide. Planta 210 (1), 115–125.
Meng, F.C., Zhang, J.H., Yao, F.M., Hao, C., 2014. Interactive effects of elevated CO_2 concentration and irrigation on photosynthetic parameters and yield of maize in northeast china. PLoS One 9 (5), 1–13.
Mo, X.G., 1997. A model for the relationship between canopy surface resistance and environmental factors and its application to evapotranspiration estimation. Geogr. Res. 2, 82–89 (in Chinese with English abstract).
Monteith, J.L., 1965. Evaporation and environment. In: Fogg, B.D. (Ed.), The State and Movement of Water in Living Organism. Symposia Soc. Exp. Biol. pp. 205–234.
Morison, J.I.L., 1987. Intercellular CO_2 concentration and stomatal response to CO_2. In: Zeiger, E., Farquhar, G.D., Cowan, I.R. (Eds.), Stomatal Function. Stanford University Press, Stanford, CA, pp. 229–251.
Morison, J.I.L., 1998. Stomatal response to increased CO_2 concentration. J. Exp. Bot. 49, 443–452.
Morison, J.I.L., Gifford, R.M., 1983. Stomatal sensitivity to carbon dioxide and humidity. A comparison of two C_3 and two C_4 grass species. Plant Physiol. 71, 789–796.
Neitsch, S.L., Arnold, J.G., Kiniry, J.R., Williams, J.R., King, K.W., 2005. Soil and water assessment tool theoretical documentation. Version 2005 edn., Grassland, soil and research service. Temple, TX.
Niu, J., Sivakumar, B., Chen, J., 2013. Impacts of increased CO_2 on the hydrologic response over the Xijiang (West River) basin, South China. J. Hydrol. 505, 218–227.
Noilhan, J., Planton, S., 1989. A simple parameterization of land surface processes for meteorological models. Mon. Weather Rev. 117 (3), 536–549.
Piao, S.L., Ciais, P., Huang, Y., Shen, Z.H., Peng, S.S., Li, J.S., Zhou, L.P., Liu, H.Y., Ma, Y.C., Ding, Y.H., Friedlingstein, P., Liu, C.Z., Tan, K., Yu, Y.Q., Zhang, T.Y., Fang, J.Y., 2010. The impacts of climate change on water resources and agriculture in China. Nature 467, 43–51.
Reckmann, U., Scheibe, R., Raschke, K., 1990. Rubisco activity in guard cells compared with the solute requirement for stomatal opening. Plant Physiol. 92, 246–253.
Rogers, H.H., Sionit, N., Cure, J.D., Smith, J.M., Bingham, G.E.B., 1984. Influence of elevated carbon dioxide on water relations of soybeans. Plant Physiol. 74 (2), 233–238.
Ruiz-Vera, U.M., Siebers, M., Gray, S.B., Drag, D.W., Rosenthal, D.M., Kimball, B.A., Ort, D.R., Bernacchi, C.J., 2013. Global warming can negate the expected CO_2 stimulation in photosynthesis and productivity for soybean grown in the Midwest United States. Plant Physiol. 162, 410–423.
Ruiz-Vera, U.M., Siebers, M.H., Drag, D.W., Ort, D.R., Bernacchi, C.J., 2015. Canopy warming caused photosynthetic acclimation and reduced seed yield in maize grown at ambient and elevated [CO_2]. Global Change Biol. 21, 4237–4249.
Schmid, I., Franzaring, J., Müller, M., Brohon, N., Calvo, O.C., Högy, P., Fangmeier, A., 2016. Effects of CO_2 enrichment and drought on photosynthesis, growth and yield of an old and a modern barley cultivar. J. Agron. Crop Sci. 202 (2), 81–95.
Shi, Z.Q., 1995. Advances of studies on carbon metabolism in guard cells (Review). Acta Agric. Univ. Pekinensis 21, 94–100 (in Chinese with English abstract).
Sicher, R.C., Bunce, J.A., 1999. Photosynthetic enhancement and conductance to water vapor of field-grown *Solanum tuberosum* (L.) in response to CO_2 enrichment. Photosynth. Res. 62, 155–163.
Silva, J.B.L.D., Ferreira, P.A., Pereira, E.G., Costa, L.C., Miranda, G.V., 2012. Development of experimental structure and influence of high CO_2 concentration in maize crop. Eng. Agríc. 32 (2), 306–314.
Stewart, J.B., 1988. Modeling surface conductance of pine forest. Agric. For. Meteorol. 43 (1), 19–35.
Sun, J.W., Zhao, T.H., Fu, Y., Zhao, Y.X., Shi, Y., 2009. Effects of Elevated CO_2 concentration on photo-physiological characteristics of maize leaves. J. Maize Sci. 17 (2), 81–85 (in Chinese with English abstract).
Tanasijevic, L., Todorovic, M., Pereira, L.S., Pizzigalli, C., Lionello, P., 2014. Impacts of climate change on olive crop evapotranspiration and irrigation requirements in the Mediterranean region. Agric. Water Manage. 144, 54–68.
Tao, F.L., Yokozawa, M., Zhang, Z., 2009. Modelling the impacts of weather and climate variability on crop productivity over a large area: a new process-based model development, optimization, and uncertainties analysis. Agric. For. Meteorol. 149, 831–850.
Thom, A.S., 1972. Momentum, mass and heat exchange of vegetation. Q. J. R. Meteorol. Soc. 98 (415), 124–134.
Tourula, T., Heikinheimo, M., 1998. Modelling evapotranspiration from a barley field over the growing season. Agric. For. Meteorol. 91, 237–250.
Tuba, Z., Szente, K., Koch, J., 1994. Response of photosynthesis, stomatal conductance, water use efficiency and production to long-term elevated CO_2 in winter wheat. J. Plant Physiol. 144 (6), 661–668.
van Bavel, C.H.M., 1974. Antitranspirant action of carbon dioxide on intact sorghum plants. Crop Sci. 14 (2), 208–212.
Vanaja, M., Yadav, S.K., Archana, G., Lakshmi, N.J., Reddy, P.R.R., Vagheera, P., Razak, S.K.A., Maheswari, M., Venkateswarlu, B., 2011. Response of C_4 (maize) and C_3 (sunflower) crop plants to drought stress and enhanced carbon dioxide concentration. Plant Soil Environ. 57 (5), 207–215.
Vu, J.C.V., Allen, L.H., 2009. Growth at elevated CO_2 delays the adverse effects of drought stress on leaf photosynthesis of the C4 sugarcane. J. Plant Physiol. 166 (2), 107–116.
Wall, G.W., Brooks, T.J., Adam, N.R., Cousins, A.B., Kimball, B.A., Pinter, P.J., LaMorte, R.L., Triggs, J., Ottman, M.J., Leavitt, S.W., Matthias, A.D., Wiliams, D.G., Webber, A.N., 2001. Elevated atmospheric CO_2 improved *Sorghum* plant water status by ameliorating the adverse effects of drought. New Phytol. 152, 231–248.
Wall, G.W., Garcia, R.L., Wechsung, F., Kimball, B.A., 2011. Elevated atmospheric CO_2 and drought effects on leaf gas exchange properties of barley. Agric. Ecosyst. Environ. 144, 390–404.
Wand, S.J.E., Midgley, G.F., Jones, M.H., Curtis, P.S., 1999. Responses of wild C4 and C3 grass (Poaceae) species to elevated atmospheric CO_2 concentration: a meta-analytic test of current theories and perceptions. Global Change Biol. 5, 723–741.
Wang, R.Y., Bowling, L.C., Cherkauer, K.A., Cibin, R., Her, Y., Chaubey, I., 2016. Biophysical and hydrological effects of future climate changeincluding trends in CO_2, in the St. Joseph River watershed, Eastern Corn Belt. Agric. Water Manage. 180, 280–296.
Wang, J.L., Wen, X.F., 2010. Modeling the response of stomatal conductance to variable CO_2 concentration and its physiological mechanism. Acta Ecol. Sin. 30 (17), 4815–4820 (in Chinese with English abstract).
Wang, J.L., Yu, G.R., Wang, B.L., Qi, H., Xu, Z.J., 2005. Response of photosynthetic rate and stomatal conductance of rice to light intensity and CO_2 concentration in northern China. Acta Phytoecol. Sin. 29 (1), 16–25 (in Chinese with English abstract).
Wijewardana, C., Henry, W.B., Gao, W., Reddy, K.R., 2016. Interactive effects on CO_2, drought, and ultraviolet-B radiation on maize growth and development. J. Photochem. Photobiol. B: Biol. 160, 198–209.
Wilson, K.B., Carlson, T.N., Bunce, J.A., 1999. Feedback significantly influences the simulated effect of CO_2 on seasonal evapotranspiration from two agricultural species. Global Change Biol. 5, 903–917.
Wu, Y., Liu, S., Abdul-Aziz, O.I., 2012. Hydrological effects of the increased CO_2 and

climate change in the Upper Mississippi River Basin using a modified SWAT. Clim. Change 110 (3–4), 977–1003.
Xie, Y.T., 2013. Effect of Free Air CO_2 Enrichment and Free Air Temperature Increase on Growth and Yield in Wheat. Dissertation for the Master Degree. Nanjing Agricultural University, Nanjing, pp. 161.
Xu, Y.J., Jing, Y.S., You, E., Ma, Y.P., Li, S.K., 2014. Effect of elevated atmospheric CO_2 concentration on leaf characteristic and evapotranspiration in winter wheat. Sci. Technol. Eng. 14 (2), 17–22 (in Chinese with English abstract).
Yu, Y.L., 2015. Effect of CO_2 Elevation on Wheat Growth and Water Utilization. Dissertation for the Master Degree. China Agricultural University, Beijing, pp. 48.
Yu, G.R., Wang, Q.F., 2010. Ecophysiology of Plant Photosynthesis, Transpiration, and Water Use. Science Press, Beijing (in Chinese).
Zhang, B.Z., Kang, S.Z., Li, F.S., Zhang, L., 2008. Comparison of three evapotranspiration models to Bowen ratio-energy balance method for a vineyard in an arid desert region of northwest China. Agric. For. Meteorol. 148 (10), 1629–1640.
Zheng, F.Y., Peng, S.L., 2001. Meta-analysis of the response of plant eco-physiological variables to doubled atmospheric CO_2 concentration. Acta Bot. Sin. 43 (11), 1101–1109 (in Chinese with English abstract).
Ziska, L.H., Bunce, J.A., 1997. Influence of increasing carbon dioxide concentration on the photosynthetic and growth stimulation of selected C_4 crops and weeds. Photosynth. Res. 54 (3), 199–208.